

# Increasing the self-sufficiency of a university campus by expanding the PV capacity while minimizing the energy cost

Tina Arizo Randrianantenaina<sup>1</sup>, Josselin Le Gal La Salle<sup>1</sup>, Sergiu Viorel Spataru<sup>2</sup> , and Mathieu David<sup>1,\*</sup> 

<sup>1</sup> University of La Reunion – PIMENT Laboratory, 15 avenue René Cassin, 97715 Saint-Denis, La Reunion, France

<sup>2</sup> Department of Electrical and Photonics Engineering, Technical University of Denmark, Roskilde, Denmark

Received: 29 September 2024 / Accepted: 3 December 2024

**Abstract.** Microgrids, which promote the production and consumption of renewable energy on site, are a relevant solution to reduce carbon emissions and the price of energy for end users. However, converting an existing building stock into a microgrid powered mainly by renewable energy requires finding a technical and economic optimum while taking into account strong constraints. This work proposes a methodology to achieve this objective on an existing university campus located in La Reunion, a French island in the Indian Ocean. The campus already has three photovoltaic (PV) systems and high-quality measurement data of weather, loads and energy production. The goal of the work is to find an optimal rooftop PV capacity that maximizes campus self-sufficiency while keeping energy price affordable for users. The results do not highlight a unique combination of roofs as a solution to the optimization problem. However, the analysis of possible combinations gives clear rules for defining the total photovoltaic capacity to be installed and selecting the most suitable roofs.

**Keywords:** Microgrid / self-sufficiency / cost of energy / optimization / PV capacity expansion  
PV system modelling

## 1 Introduction

This work is motivated by the urgent necessity to advance sustainable and resilient energy systems, driven by global environmental and energy challenges. Finding the optimal techno-economic strategy has become a critical scientific problem. Microgrids, known for their ability to operate independently or connected to the main grid, have emerged as a promising solution to tackle these challenges [1]. They offer the potential to transform the energy landscape by enhancing self-sufficiency of prosumers, decreasing reliance on fossil fuels, and ultimately mitigating the impacts of greenhouse gas emissions on the environment. A microgrid is a small-scale electrical power system that can operate either connected to or independent from the main power grid. Microgrids are characterized by their ability to generate, distribute, and manage power locally, while also being able to exchange power with the main grid [2]. Among the different categories of microgrids, we will focus in this work on a microgrid that is connected to the main grid and relies on a mix of local and external energy sources. This type of microgrid system is able to export any excess energy back to the main grid and buy energy from the grid

when the local generation is insufficient [3]. The microgrid is the university campus of Terre Sainte, located in La Reunion, a small island of the Indian Ocean, close to the Capricorn tropic. It already has rooftop photovoltaic (PV) arrays and a diverse range of electrical and thermal loads. The various systems (i.e. buildings, cooling coils, PV rooftops, etc.) of this microgrid, combined with its geographical location on an island, present an intriguing and multifaceted research opportunity. Self-sufficiency is a key objective in grid-connected microgrids as it promotes energy independence. The level of self-sufficiency is defined as the ratio between the energy produced by onsite renewable energy systems and the energy used onsite by the microgrid and can be calculated every time step or for a full cycle like a year. The higher the self-sufficiency, the lower the energy exchange with the main grid, leading to greater energy independence. However, increasing self-sufficiency is not always an affordable solution.

Several works have already proposed solution to increase the self-sufficiency of university campuses with the integration of various renewable energies. Akindeji et al. [4] focus on minimizing fuel costs and CO<sub>2</sub> emissions while increasing reliance on renewable energy in a hybrid renewable energy system (HRES) for university campuses. Their work considers seasonal variations in solar and wind energy to integrate solar PV, wind turbines, and battery

\* e-mail: [mathieu.david@univ-reunion.fr](mailto:mathieu.david@univ-reunion.fr)

storage, with a diesel generator as backup. Although fuel savings were achieved, installation and energy costs were not assessed. In another work, Akindeji et al. [5] aims to maximize utility bill savings and minimize CO<sub>2</sub> emissions at the University of KwaZulu-Natal (UKZN) in South Africa, using a hybrid system that combines the national grid, solar PV, wind, and battery systems to address frequent power failures and load shedding. Their work proposes a methodology to reach an optimal combination of renewable sources, grid supply and energy storage. A case study at Beirut Arab University implemented a 500 kWp solar microgrid with diesel generators to improve campus sustainability. The system supplied 67% of the energy demand during winter days, proving to be an effective solution for cost and emission reductions [6]. Another study at a Saudi Arabian university campus proposed a hybrid microgrid design combining solar PV and wind energy. The system generated 3.27 GWh annually, with a renewable fraction of 3.7%. The wind system had a higher capacity factor and longer payback period compared to the PV system. Their complementarity results in a balance between efficiency and economic feasibility [7]. Finally, the smart campus microgrid at Hellenic Mediterranean University (HMU) in Crete utilizes PV systems, wind turbines, and battery storage to increase renewable energy capacity. The study demonstrates financial feasibility and load reduction, with HMU's investment proving more sustainable than similar projects in northern Europe, largely due to the favorable Mediterranean climate [8]. A previous work of Sanchez [9] on the Terre Sainte campus microgrid explores increasing energy self-sufficiency to 80% by simulating solar PV, wind turbines, and battery storage. The study finds that combining PV and wind reduces reliance on batteries but requires a higher initial investment. While PV and wind offer greater long-term energy yields, PV alone is more financially viable due to lower upfront costs. Although these studies achieved optimal results for hybrid systems, they did not address critical details needed for modeling PV systems, such as roof type, grid connection, and orientation. Moreover, even if the proposed designs lead to increase renewable capacity and reduction of operation cost, the affordability for the users is rarely studied. Finally, most of these works are based on fictive systems inspired by real campuses and many simplifying hypothesis are made due to the lack of data.

The University campus of Terre Sainte, which has a comprehensive and high-quality measurement data set, is an ideal case study to contribute addressing some of these lacks in the literature. In this work, we focus on testing a methodology to aid decision making to increase self-sufficiency with additional rooftop PV capacity while minimizing the cost of self-consumed energy of an existing microgrid. No flexibility means, such as energy storage or demand management, will be considered to assess the extent to which PV capacity alone will contribute to our objectives. Since the buildings are already existing, the available surface area and roof characteristics (materials, slope, orientation, etc.) are strong constraints to find an optimal solution. However, due to the large variety of roof slopes and orientations available on campus, we assume

that a combination will likely optimize both of our objectives, i.e. maximizing self-sufficiency and minimizing energy cost, simultaneously. This work proposes to address two main challenges to validate this assumption. First, we develop accurate modeling of the production of existing and future photovoltaic systems, leveraging existing data. Second, we propose an optimization framework, taking into account both technical and economic factors, to simultaneously evaluate the effect of possible roof combinations on self-sufficiency and energy cost.

The paper consists of several key sections. In the next section, the methodology describes the research approach. Then, Section 3 introduces the campus microgrid and on-site data. In Section 4, we detail how we selected and validated an appropriate model to simulate current and future PV systems. Section 5 presents the multi-objective optimization used to find the best combination of rooftop PV systems that simultaneously maximize self-sufficiency and minimize energy cost. The results are discussed in Section 6. The paper ends with concluding remarks and outlooks that summarize the results and suggest future directions.

## 2 Methodology

The methodology employed in this work aims to select the best combination of PV systems to increase the self-sufficiency while keeping the cost of electricity affordable for the users. It involves a systematic approach consisting of three key steps:

- We collected and consolidated the required data to model and optimize the PV capacity. Data was recorded onsite with a weather station and energy meters, which monitor building electricity demand and PV production. We also identified and assessed the available rooftop areas to determine the potential for expanding the PV capacity.
- We developed a model to simulate the future PV production. To evaluate the accuracy of the results, we validated the model with the actual PV productions.
- We defined an optimization framework to select the best combination of rooftop PV systems and corresponding PV capacities. For this last step, we used a multi-objective optimization based on two complementary cost functions. The first one gives the cost of energy for the users of the microgrid and the second the level of self-sufficiency. Finally, we performed a Pareto front analysis to evaluate the features that allow selecting an optimal configuration, balancing both cost efficiency and energy self-sufficiency objectives.

This comprehensive methodology ensures a reliable foundation and informed decision-making to meet the work's objectives effectively.

## 3 The university campus of Terre Sainte and available data

The university campus of Terre Sainte located on the coastal part of La Reunion (21°20'S, 55°29'E), which is an island situated in the southern part of the Indian Ocean, is

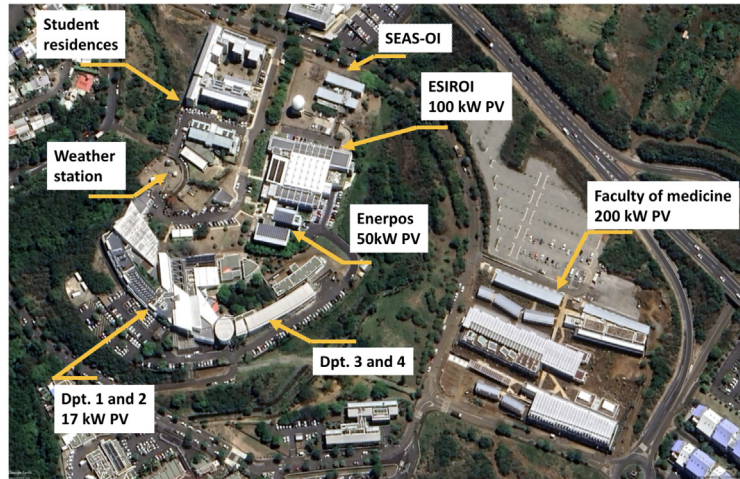


Fig. 1. Overview of the university campus of Terre Sainte, La Reunion.

Table 1. Key figures of the Terre Sainte campus.

Building name	Commissioning year	Floor area (m <sup>2</sup> )	Electricity demand 2021 (kWh)	Installed PV (kWp)	Potential additional PV (kWp)
Dpt. 1 and 2	1998	5,006	273,432	17	373.4
Dpt. 3 and 4	2006	2,171	228,309	–	223.0
Enerpos	2008	979	15,710	49.1	46.9
SEAS-OI	2012	597	34,178	–	72.0
ESIROI	2020	3,885	260,160	100	127.9
Student residences	2008 and 2019	6,110	373,060	–	173.0
Faculty of Medicine	2023	–	–	200	–
<b>Total</b>		<b>18,748</b>	<b>1,184,759</b>	<b>166.1</b>	<b>1,016.2</b>

a grid-connected microgrid. It consists of rooftop solar PV systems, electrical and thermal loads. The climate is hot and humid during the wet season (Nov. to Apr.) and cooler with trade winds during the dry season (Apr. to Nov.). The annual solar potential of the site reaches 2000 kWh m<sup>-2</sup> on a horizontal surface, making it an ideal location for using solar PV. The campus hosts more than 1000 students and is made up of eight groups of buildings divided into student residences, university buildings and a restaurant. There are three operational PV plants, and a fourth one has been recently installed on the roof of the Faculty of Medicine. Figure 1 and Table 1 give an overview of the campus buildings and existing PV capacity. The Faculty of medicine, which was commissioned in September 2023, is not currently included in the scope of the microgrid because we do not have any data. This work is based on a set of consolidated data with a 10-min granularity for two consecutive years, 2021 and 2022, which gives all the information needed to study and simulate the microgrid [10]. The dataset is publicly available in the deliverables section of the website of the European project TwInSolar [11].

### 3.1 Existing on-site production systems

The university buildings currently host 3 PV systems on their roofs for a total capacity of approximately 160 kWp.

An additional capacity of 200 kWp on the roofs of the faculty of medicine will come soon and it is not included in this work. An analysis of recorded electric load and PV production shows that the microgrid has an electrical self-sufficiency of nearly 16%. Table 2 gives detailed information about the solar power setups on the campus. The ENERPOS building has a total peak power of 49.14 kWp, with two well-ventilated arrays (18.9 kWp and 30.24 kWp) commissioned in 2008. The ESIROI building, with a total peak power of 99.935 kWp, features two arrays (68.335 kWp and 31.6 kWp) commissioned in 2021. The Dpt. 1 and 2 buildings has a total peak power of 11.385 kWp, with a single rack-mounted array commissioned in 2006.

The production of the different PV plants is recorded by inverters from different manufacturers, resulting in data with different time resolutions. To be consistent with the load, we created a set of consolidated data with an harmonized time-step of 10-min and covering two consecutive years, 2021 and 2022. As for the weather data and the building loads, the PV production data is publicly available on the TwInSolar website [11].

### 3.2 Available surfaces to extend PV capacity

To determine available space for solar power system expansion, a comprehensive approach was employed,

**Table 2.** Key figures of the 3 existing PV systems.

	Dpt. 1 & 2	ENERPOS	ESIROI
Module technology	Multi-Si	Multi-Si	Mono-Si
Module STC* power (W)	165	210	395
Module STC* efficiency	0,127	0,14	0,203
Total DC power (kW)	11.385	49.14	99.935
Orientation and slope	0° North, 21°	14° NE, 9° (18.9 kW) 194° SW, 9° (30.24 kW)	14° NE, 30° (68.335 kW) 103° SE, 16° (31.6 kW)
Total inverter AC power (kW)	11	50	106
Inverter peak efficiency	0.941	0.983	0.987
Commissioning year	2006	2008	2021

integrating Google Maps measurement tool, the Helioscope software [12], and real dimensions measured on building plans. Helioscope, renowned for its sophisticated solar design capabilities, played a pivotal role in this process. Its graphical web-based interface facilitates roofs' azimuth estimation and PV panel layout, allowing the estimation of the maximum number of PV modules that can be installed on the existing roofs. For expansion simulations, we chose the Sunpower MAXEON 3 400W module for its advanced technology and compatibility with standard PV modules used in La Reunion. Safety and accessibility were prioritized, with a one-meter buffer maintained around the roof for maintenance activities and strategic gaps every thirty meters to enhance safety and streamline logistics. This meticulous approach ensures the longevity and efficiency of the solar power system, aligning with sustainability goals and effective energy solutions. The campus has 39 available roofs, including 9 flat roofs with an available area of approximately 1200 m<sup>2</sup>, and 31 sloping roofs with an available area of around 5,600 m<sup>2</sup>. The pitched roofs present a wide variety of slopes, ranging from 6° to 22°, and azimuths covering all the main orientations (North, East, South, and West).

Our aim is not to increase the PV capacity to its maximum but to design a solution for an affordable electricity supply. Thus, we do not wish to use all the available roofs but to select the most suitable ones.

### 3.3 Weather station

The campus has its own weather monitoring system equipped with advanced solar sensors. First, a weather station, which complies with the World Meteorological Organisation (WMO) standards, records the air temperature, relative humidity, barometric pressure, rainfall, wind speed and direction. Second, a two axis Kipp & Zonen solar tracker measures with class A sensors different components of solar irradiance such as normal direct (DNI), diffuse horizontal (DIFH), global horizontal (GHI) and horizontal infrared (IR). In case of failure of the tracker, the weather monitoring system also has a SPN1, which is a sensor that measures GHI and DIFH without rotating piece. Even if its accuracy is slightly lower than the class A pyranometers mounted on the tracker, it is a good backup system that

ensure the continuity of the times series of irradiance. All these weather and solar data are very important to accurately simulate the production of the PV systems installed onsite. The original sampling period of the weather data is 1 minute. To have a common time step with the PV production and building loads, we did the 10 minutes mean of the data.

We applied a quality check (QC) procedure to the solar irradiance data, which is the primary variable influencing the PV production. Among the various available QC, we used the QC procedure recommended by the Baseline Surface Radiation Network [13] because it is commonly used by the scientific community to test observed solar data [14] and its implementation is very well described in the Jupyter Notebook proposed by Jensen and Saint-Drenan [15]. Figure 2 presents the first test of the procedure for the 3 components of solar irradiance measured with the solar tracker. Valid measurements must be below the green and red lines that gives the physical possible limit and the extremely rare limit respectively. We can easily see that the 2 years of solar data fully comply with these limits.

The other tests proposed in [15] were applied to the data and they confirmed the high quality of the recorded solar data. The only test that is not completely validated is the 3 components comparison, also called closure equation test. It shows that combining DIFH and DNI to compute the GHI leads to a slight overestimation of the measured GHI.

### 3.4 Loads

The campus has a floor area of 18,750 m<sup>2</sup> with university buildings, a student residence with 244 rooms, and a restaurant. With a third of their floor area equipped with air-conditioning, the main load of the university buildings is the cooling. The last generation of university buildings built on the campus (ENERPOS and ESIROI) are NetZero Energy Buildings [16]. Designed on bioclimatic principles, their energy needs are lower than classical buildings and they integrate rooftop PV systems to balance their electricity consumption. The student residences are already equipped with solar domestic hot water (DWH) that supplies more than 80% of the energy needed. The campus also has electric vehicles chargers (4 plugs for a total of 88 kW) but they do not represent a significant share

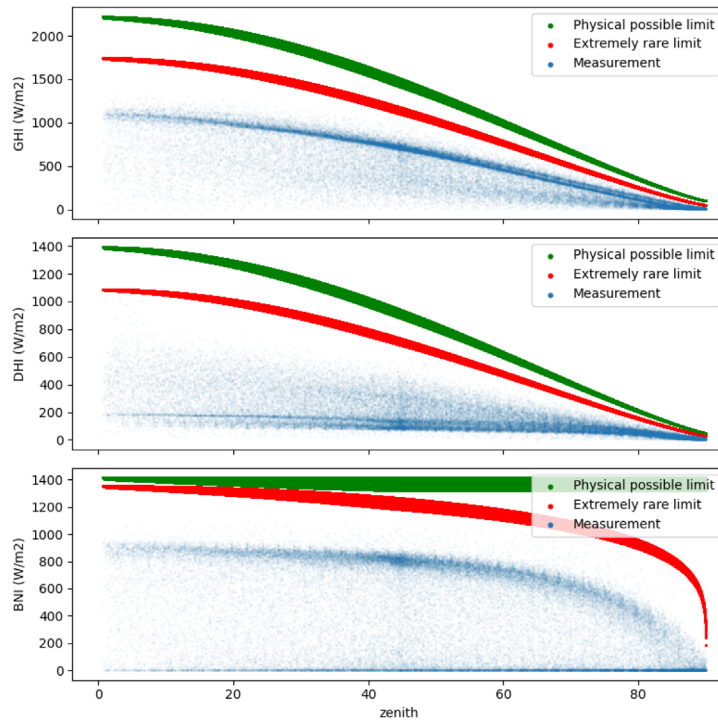


**Fig. 2.** Quality Check of the 3 components of solar irradiance (GHI, DNI and DIFH), verification of compliance with extremely rare limit and physically possible limit.

of the total load. Thus, the campus loads are exclusive electric and they are dominated by cooling demand. Table 1 gives the electric consumption of each building group for the year 2021.

The campus has a total electricity consumption of approximately 1.2 GWh in 2021. The overall shape of the load profile presented in Figure 3 shows that the energy demand occurs primarily during daylight hours. Therefore, powering the microgrid with solar energy seems to be a good solution to increase its self-sufficiency. However, with a relatively important share of demand occurring at night, a solution based solely on solar energy will have its limitations.

The campus microgrid electricity demand and production are currently recorded by the local distribution system operator, EDF Reunion. This company records the energy produced and the power generated by each installation on every transformer. We receive the annual energy load and production data, provided in 10-minute intervals. The electricity demand is recorded for each building separately and for the most recent constructions, the main types of loads (i.e., cooling, lights, ceiling fans, etc.) are also monitored.

## 4 PV system model

In this section, we present the models and tools used to simulate the PV systems. We also provide a comparison with the data recorded on the existing PV plants.

### 4.1 Modeling tools

Our modeling relies on two well-regarded tools: the System Advisor Model (SAM) [17] and the pvlib library [18].

SAM, developed by the National Renewable Energy Laboratory (NREL), is a software package designed for comprehensive financial and performance modeling of renewable energy systems, including PV [19]. It offers a user-friendly interface and extensive databases for system components and weather data [17]. At the heart of SAM lies a suite of physical models that predict various aspects of PV system's performance. These models tackle critical factors like solar radiation. Here, SAM predicts the amount of sunlight striking the tilted surface of the PV modules throughout the year, considering both location and historical weather data. Additionally, SAM incorporates performance models specific to different module types [19]. This allows estimating electricity generation based on the incoming solar radiation and the ambient temperature. Inverter efficiency is another crucial aspect considered. Inverter models account for power losses that occur during the conversion of DC electricity from the modules to AC electricity for grid connection. Finally, SAM factors in various DC and AC losses within the system. These include losses due to soiling, mismatch between modules, wiring resistance, connection points, and even aging (which can be user-defined). By combining weather data, these physical models, and the user-defined system characteristics, SAM simulates the hourly or daily electricity production of the PV system throughout a chosen period, typically a year. However, SAM has limitations. For instance, we can only include a maximum of 4 subarrays to an inverter and only one type of module and inverter per plant. Additionally, the time resolution of its outputs is limited to a 1-hour time step.

On the other hand, pvlib is a Python-based open-source library [18]. It provides a collection of well-documented functions for modeling individual aspects of PV systems,

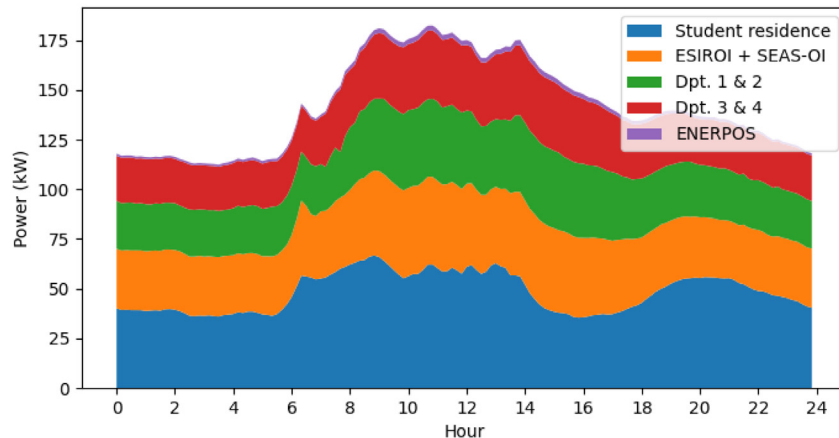


**Fig. 3.** Average annual load profile of the different buildings on the Terre Sainte campus.

such as solar radiation, electrical performance, and inverter losses [20]. This modular approach offers greater flexibility for customization. However, pvlib requires users to write their own Python codes and to manage data inputs, making it less user-friendly for beginners. The PVWatts calculator created by the National Renewable Energy Laboratory is integrated into the pvlib library. It allows users to predict the electricity output of a solar power system connected to the grid by requiring only a minimal amount of data as input [21,22]. We used an isotropic sky model to compute the amount of solar radiation striking the tilted surface of the modules throughout the year based on location and historical weather data. Additionally, it considers the type of modules used and their efficiency curves to estimate electricity generation based on incoming sunlight, ambient temperature and wind speed. Inverter efficiency is also factored in, accounting for power losses during the conversion of DC electricity from the modules to AC electricity for grid connection. Finally, user-defined values for DC and AC losses (soiling, mismatch, wiring, etc.) are integrated into the calculations. By combining weather data, these internal models, and user-specified system characteristics, PVWatts estimates electricity production of the PV system over a chosen period, typically a year.

## 4.2 Simulation of existing PV systems

The validation process of a model relies on a meticulous performance assessment, where the model's adherence to measured trends determines its reliability. This assessment involves conducting simulations with the same meteorological input data as on-site measurements, enabling a direct comparison between simulated and measured energy production. To ensure the accuracy of results, a comprehensive data analysis is performed, necessitating data filtering to address missing inputs and detect outliers.

To objectively compare SAM and pvlib results, we have not used their predefined component libraries. We modeled the existing PV systems with the parameters given by the datasheets of inverters and modules manufacturers detailed in Table 2. With the same objective, we used the same weather data as an input of both tools. Indeed, while SAM offers a comprehensive library of pre-defined

weather data, modules and inverters, the specific models used in our existing system were not available. Therefore, we manually entered their characteristics into the software for accurate simulation. For pvlib, we created a custom CEC model based on the manufacturer's datasheet. Both models incorporated identical Direct Current (DC) loss values to account for various factors: soiling loss 1%, mismatch loss 1%, wiring loss 1%, connection loss 0.5%, aging loss 0.5%/year and nameplate loss 0%.

The pvlib and SAM's models were tested and compared with actual data from the three existing systems (ENERPOS, ESIROI, and Dpt. 1 & 2). Figure 4 shows the comparison between the actual monthly production, the results of the pvlib and SAM simulations for the three buildings considered. The shapes of the three plots demonstrate that both models reproduce accurately the trends observed in the actual system. This strengthens the idea that these models can be used to simulate new systems for the available roofs on the campus.

The comparison between produced and simulated energy involves the use of error metrics to quantify the deviation between measured and modeled data. For each existing system, the accuracy is assessed by the mean bias error (MBE) and the root mean square error (RMSE) defined as follow:

$$MBE(\%) = \frac{\frac{1}{n} \sum (x_{model} - x_{true})}{\frac{1}{n} \sum (x_{true})} \times 100 \quad (1)$$

$$RMSE(\%) = \frac{\sqrt{\frac{1}{n} \sum (x_{model} - x_{true})^2}}{\frac{1}{n} \sum (x_{true})} \times 100. \quad (2)$$

The MBE represents the average bias and the systematic tendency of the model to under or overestimate [23]. The RMSE is the square root of the variance of the residuals. It is strongly influenced by the high deviations of the models. It evaluates how well the model can fit and predicts reality.

The errors calculations for each building are presented in Table 3. Notably, the results indicate satisfactory agreement between both models. Considering the satisfying alignment

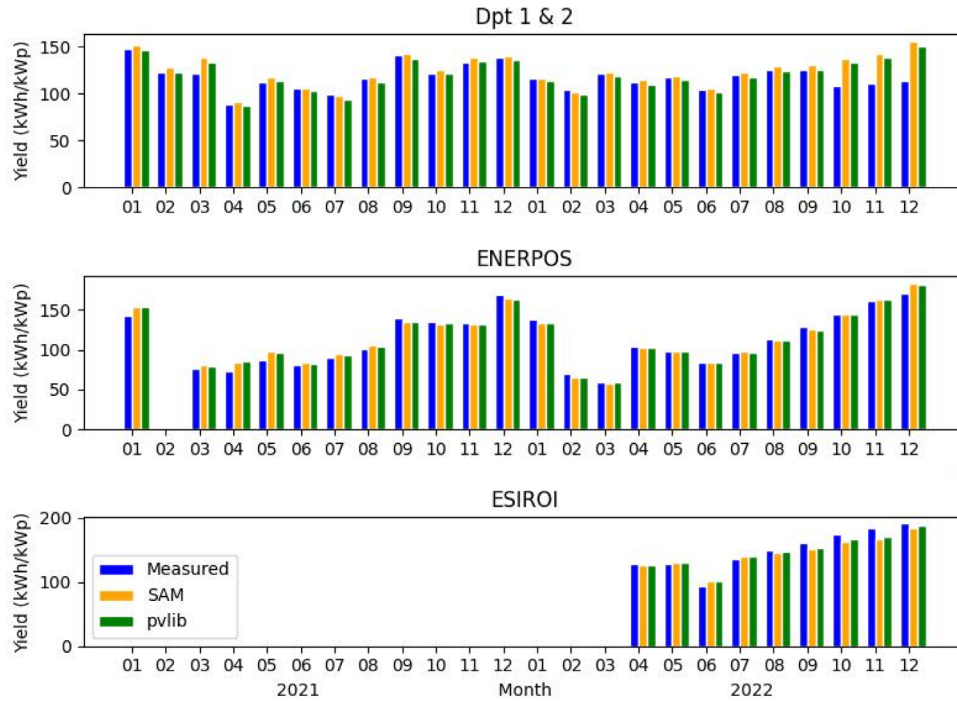


Fig. 4. Comparison of the measured monthly yield with the simulations done with SAM and pvlb.

Table 3. Error in PV production of the two tested models (SAM and pvlb) for the 3 existing rooftop PV systems.

		ENERPOS	ESIROI	Dpt. 1 & 2
MBE (%)	SAM	-0.57	0.42	6.48
	pvlb	-0.31	-0.36	5.12
RMSE (%)	SAM	12.61	8.72	14.72
	pvlb	0.18	12.65	24.04

between the measured and simulated data, particularly the low MBE for ENERPOS and ESIROI, we can assert that the models are trustworthy. However, we chose the pvlb library for the optimization step because it is more flexible and easier to automate.

### 4.3 Simulation of additional PV capacity

To simulate the additional PV capacity, we used the model (i.e. PVWatts) and parameters (i.e. losses) defined to simulate the existing systems. We decided to lead a uniform approach using a single high-performing solar panel. We obviously used the same model as that chosen to define the number of modules that can be installed on the roofs (see Sect. 3.2): the Sunpower MAXEON 3, 400W.

For PV cell temperature modeling, we used two configurations of the Sandia Array Performance Model (SAPM) implemented in the pvlb library [24], ‘close mount glass glass’ and ‘open rack glass polymer’ depending on whether the installation was mounted directly on a roof or on a rack. We included both tilted and flat roofs in our simulations, but shading effects were not considered.

For inverters, we modeled a generic inverter for each rooftop with a nominal power equal to the installed PV power. This inverter model represents a scenario with variable yield and has a high efficiency of 98%. The output provides AC power for each roof on a 10-minute time step.

## 5 Optimization

The optimization problem aims to maximize self-sufficiency of the microgrid while minimizing investment costs of increasing the PV capacity on available rooftops of the campus. This multi-objective optimization is based on two objective functions, also called cost functions. The first one is the self-sufficiency rate of the microgrid. It quantifies the share of the total load that is supplied by the local energy production from the PV systems installed on the roof. Self-sufficiency is the ratio between the PV production directly consumed by the microgrid and the total energy consumption.

The second objective function is the cost of the energy produced onsite by the PV plant for the microgrid operator, which is also the user in our case. In other words, it estimates the price of each kWh of the PV production

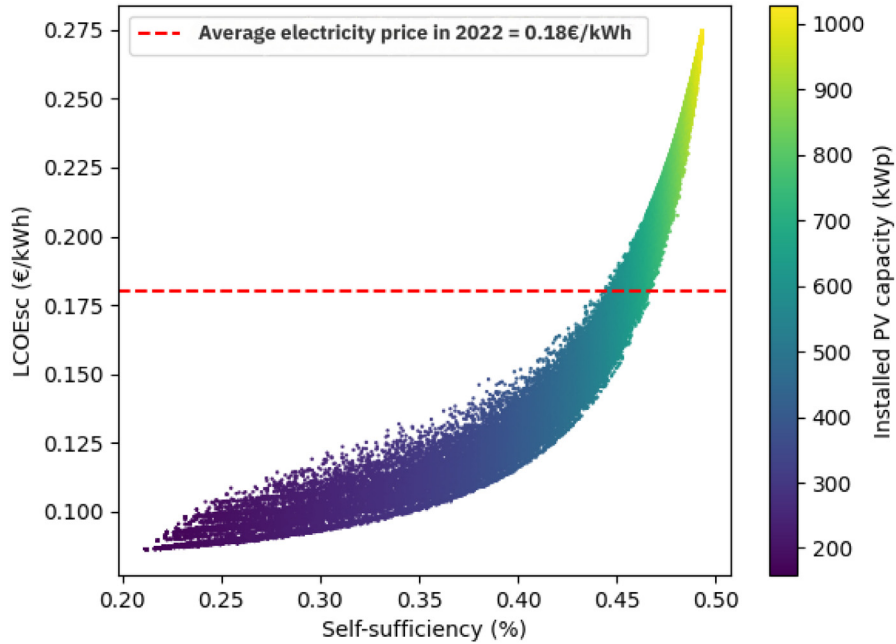


**Fig. 5.** Results of multi-objective optimization with total installed power highlighted by the color scale.

that is directly consumed by the microgrid. Therefore, in this cost function, we do not consider any selling of the energy excess that could flow to the electricity grid. We named this cost function Levelized Cost Of self-consumed Energy (LCOEsc), which is a modified version of the well-known Levelized Cost Of Energy (LCOE) [25]. It depends on the investment cost (CAPEX), the maintenance and operation costs (OPEX), the life-time of the PV system ( $LT$ ) and the PV production directly consumed by the microgrid as follow:

$$\text{LCOEsc} = \frac{\text{CAPEX} + \text{OPEX} \times \text{LT}}{\text{Yearly PV production directly consumed by the microgrid}_i \times \text{LT}}. \quad (3)$$

In order to estimate the CAPEX, we carried out a survey among private entrepreneurs in La Reunion. In our case study, the installation cost in euro per watt-peak (€/Wp) depends only on the type of roof. For pitched corrugated iron roofs, the price is 1.60 €/Wp of solar capacity. This price is a global package that includes the balance of the system (BOS), the fixing rails, the installation costs, etc. Flat waterproof roofs require additional work, with a unit cost of 125 €/m<sup>2</sup> to replace the existing waterproofing membrane. Indeed, fixing the structure requires damaging the existing waterproofing coating. This is why the replacement of the waterproofing coating is systematically taken into account by suppliers in the cost of installing the PV system on flat concrete slabs. In addition, the installation of the PV system, the aluminum mounting structure and the BOS costs 1.30 €/Wp. This results in an average installation cost for the available flat roofs of 2.96 €/Wp.

As presented in Section 3.2, in addition to the three existing PV systems, the campus has 39 roofs suitable to increase the PV capacity. Considering all the possible roof

combinations, the initial optimization problem leads to find an optimum within approximately  $10^{46}$  combinations. To reduce the computation burden and knowing that different combinations will likely results in the same self-sufficiency and CAPEX, we randomly select a subset of 50,000 combinations. To ensure that the randomly selected combinations represented the variety of possible combinations, we use a 2-step process. First, we generate a uniformly distributed random variable in the range [0;1]. Second, we use this random variable as input to a binomial distribution to define the roofs that will be part of the combination. Then, we repeat the process 50,000 times to generate our set of combinations. Finally, we added the three existing PV systems to each combination to take them into account in the computation of the objective functions.

## 6 Results and discussion

The initial hypothesis of this work is that a specific combination of roofs, due to their complementarity (i.e. various azimuths and slopes) will probably make it possible to find a techno-economic optimum. The result of the 2-objective optimization is a point cloud with a Pareto front. The analysis of the Pareto front will help selecting the optimal combination of roofs and corresponding PV capacity. The best combinations of roofs exhibit high self-sufficiency and low LCOEsc. Ideally, the LCOEsc must fall below the average electricity price of electricity purchase from the grid to be considered as affordable and also profitable for the microgrid operator. This comprehensive evaluation approach prioritizes combinations that not only demonstrate cost-effectiveness but also significantly contribute to the overarching objective of enhancing self-sufficiency of the microgrid. Figure 5 presents the point

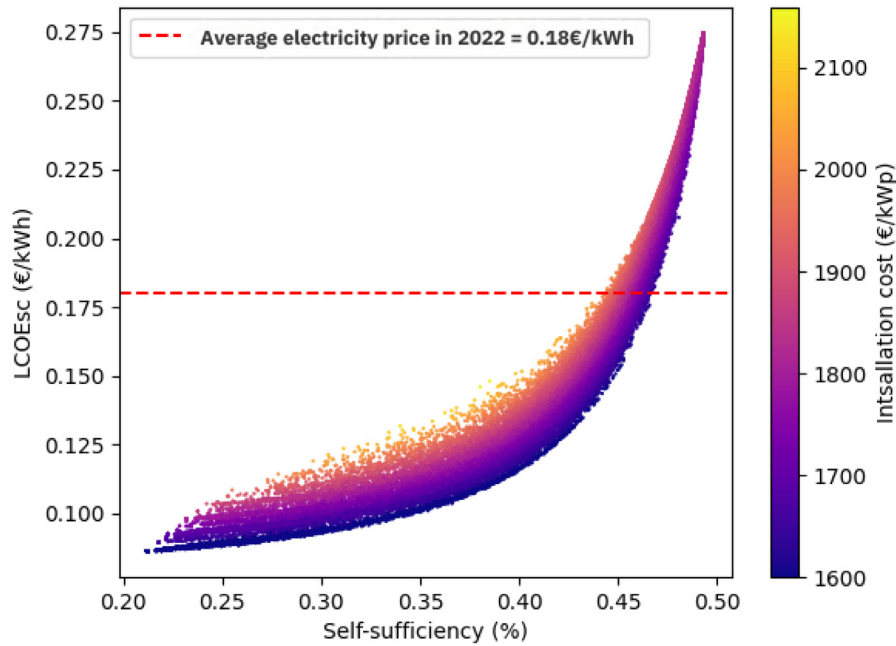


**Fig. 6.** Results of multi-objective optimization with installation cost highlighted by the color scale.

cloud with the 50,000 data points corresponding to the randomly selected roof combinations. The graph is plotted as a function of LCOEsc and self-sufficiency, and the color scale highlights the installed PV power. First of all, we note that self-sufficiency rapidly increases for installed power ranging from 160 kWp (current PV capacity) to 500 kWp and then reaches a limit close to 50%. Without means of flexibility, increasing the total installed power beyond 1 MWp will not allow this limit to be exceeded.

The interesting combinations are those below the red dashed line, which represents the average electricity price in 2022 (0.18 €/kWh), and in the outermost layer of the Pareto front, indicating higher self-sufficiency. Considering a constant LCOEsc, the color scale highlights that self-sufficiency increases with increasing PV capacity. If we zoom on the area of interest, i.e. on the right side of the point cloud and just below the red dashed line, we observe that several combinations, which present a total installed capacity of approximately 650 kWp, are good candidates. The roofs that appear most often in these interesting combinations are the largest ones. Indeed, a combination with only small roofs does not allow to reach a capacity of 650 kWp. However, with this result, it is difficult to designate a single combination as optimal.

To better understand the result of the optimization and also to find another key to select the best combination of roofs, Figure 6 presents the same point cloud as Figure 5 but with a color scale that quantifies the CAPEX. Considering a fixed self-sufficiency rate, this figure shows that LCOEsc is directly linked to the installation cost. Again, if we zoom on the area of interest below the red dashed line, one can observe that several interesting combinations have similar CAPEX. These interesting combinations consist exclusively of pitched roofs, which have lower installation costs than flat roofs.

Therefore, for this specific case study and based on the previous analysis of the optimization results, the optimal roof combinations are those involving pitched roofs with high PV power capacity, given their lower installation costs. The initial assumption that the proposed methodology would highlight a unique combination is not confirmed by the results. Even though the available roofs have a wide variety of orientations and slopes, we have not identified a set of roofs that are systematically found in the best combinations, for example, west and east facing roofs that should have increased morning and evening production. We assume that two main reasons led to this result. First, the peak load of the campus occurs in the middle of the day making the morning and evening PV production of east and west oriented panels less important to increase the self-sufficiency. Second, the campus is located in the inter-tropical zone where the sun path is high in the sky all along the year. In addition, the slopes of the pitched roof are not very important, ranging from 6° to 22°. As a consequence, the effect of orientation on the production profile is not very significant. So, it is important to note that these findings are specific to the climatic context and the layout out of the available roofs considered in the case study. We initially envisaged to also study rack mounted PV with variable slope and orientation on the 1200 m<sup>2</sup> of flat roofs. However, rack-mounted structures significantly increase the investment cost and reduce the lifetime of the waterproofing membrane. Considering the results of the optimization performed without this feature, it seems that a more expensive configuration will not lead to affordable solutions.

Finally, even if the optimization does not give a clear optimal combination of roofs, this work results in a simple guidance to select the most suitable roofs to increase the PV capacity. We can conclude that whatever

the orientations and slopes of the roofs, we must favor the least expensive ones, i.e. large pitched roofs, to achieve a total installed PV power of approximately 650 kWp. This configuration will allow us to have a self-consumed energy cost lower than the electricity grid and a self-consumption rate of 46%. As we already have 150 kWp installed, we still need to invest in an additional 500 kWp to be installed on pitched roofs.

## 7 Conclusion and perspectives

The method proposed in this work to size the additional PV capacity of the Terre Sainte campus results in clear rules for selecting the most suitable roof combinations. Without any energy storage or demand side management, a total installed PV power of 650 kWp allows to achieve a self-sufficiency of 46% with an energy cost of self-consumed PV production lower than the current price of the electricity from the grid. The initial hypothesis that a specific combination of roofs with complementary orientations and slopes should lead to an optimum has not been validated. Indeed, several combinations result in approximately the same optimum in terms of LCOE<sub>sc</sub> and self-sufficiency. For this case study, choosing roofs with the lowest installation cost is the most important.

The next step is to explore the potential of flexibility solutions, such as energy storage and demand-side management, to further increase self-sufficiency while keeping energy price as low as possible. First, demand-side management will better align energy demand and PV production at a reduced cost, but it is generally difficult to implement because it involves changing user behavior. Second, energy storage can increase self-sufficiency by shifting excess PV generation that occurs during periods of high sunlight to periods of low solar irradiance, such as at night or on cloudy days. However, adding an energy storage system will also increase the investment cost. Again, optimization is needed to select the most suitable storage technology and capacity to keep the cost of energy as low as possible while maximizing the self-sufficiency. A complementary work [26], also presented at EU PVSEC 2024, presents an optimization tool, called ERMES, which was developed to find the best design of a microgrid. It was applied to the Terre Sainte campus. With approximately the same installed PV power as defined in this article, and 900 MWh of Li-ion batteries, the microgrid can achieve self-sufficiency of over 60% and a cost of energy lower than the current average electricity price.

### Funding

This work received support from the TwInSolar project funded by the European Union under Horizon Europe (grant number 101076447).

### Conflicts of interest

The authors have nothing to disclose.

### Data availability statement

Data associated with this article are publicly accessible on the PIMENT's GitHub repository at the following link: [https://github.com/Laboratoire-Piment/TwInSolar\\_consolidated\\_data](https://github.com/Laboratoire-Piment/TwInSolar_consolidated_data).

### Author contribution statement

Conceptualization, T.A. Randrianantenaina, M. David and V.S Spataru; Methodology, T.A. Randrianantenaina, M. David and V.S Spataru; Software, T.A. Randrianantenaina; Validation, T.A. Randrianantenaina, M. David and V.S Spataru; Formal Analysis, T.A. Randrianantenaina and M. David; Investigation, T.A. Randrianantenaina; Resources, M. David; Data Curation, M. David; Writing – Original Draft Preparation, T.A. Randrianantenaina and M. David; Writing – Review & Editing, J. Le Gal La Salle and S.V. Spataru; Visualization, T.A. Randrianantenaina and M. David; Supervision, M. David and V.S Spataru; Project Administration, M. David; Funding Acquisition, M. David.

### References

1. K.M. Kelly-Pitou, A. Ostroski, B. Contino, B. Grainger, A. Kwasinski, G. Reed, Microgrids and resilience: using a systems approach to achieve climate adaptation and mitigation goals, *Electr. J.* **30**, 23 (2017). <https://doi.org/10.1016/j.tej.2017.11.008>
2. B. Kroposki, T. Basso, R. DeBlasio, Microgrid standards and technologies, in *2008 IEEE Power and Energy Society General Meeting – Conversion and Delivery of Electrical Energy in the 21st Century* (2008), pp. 1–4. <https://doi.org/10.1109/PES.2008.4596703>
3. X. Li, Y. Li, X. Li, F. Blaabjerg, Optimization of hybrid microgrid systems: a particle swarm optimization approach, *IEEE Trans. Ind. Electron.* **66**, 7096 (2019)
4. K.T. Akindeji, R. Tiako, I. Davidson, Optimization of university campus microgrid for cost reduction: a case study, *Adv. Eng. Forum* **45**, 77 (2022). <http://dx.doi.org/10.4028/p-13gc8e>
5. K.T. Akindeji, D.R.E. Ewim, Economic and environmental analysis of a grid-connected hybrid power system for a University Campus, *Bull. Natl. Res. Cent.* **47**, 75 (2023) <http://dx.doi.org/10.1186/s42269-023-01053-6>
6. M. Tarnini, M. Alsayed, A. El Ghaly, K. Chahine, Towards energy sustainability in university campuses: a case study of Beirut Arab University, *Sustainability* **15**, 7695 (2023). <http://dx.doi.org/10.3390/su15097695>
7. A. AlKassem, A. Draou, A. Alamri, H. Alharbi, Design analysis of an optimal microgrid system for the integration of renewable energy sources at a university campus, *Sustainability* **14**, 4175 (2022). <http://dx.doi.org/10.3390/su14074175>
8. A. Paspatis, K. Fiorentzis, Y. Katsigiannis, E. Karapidakis, Smart campus microgrids towards a sustainable energy transition – the case study of the hellenic mediterranean university in crete, *Mathematics* **10**, 1065 (2022). <http://dx.doi.org/10.3390/math10071065>

9. B.S. Sanchez, Modelling and optimization of a hybrid micro-grid system for maximizing energy self-sufficiency, Master Thesis, Technical University of Denmark, 2023
10. M. David, M.N. Andriamandroso, P.B. Poulsen, J. Castaing-Lasvignottes, N. Cutululis, K. Das, C. Durif-Aboukali, J. Francou, P. Lauret, J. Le Gal La Salle et al., A set of study cases for the massive integration of solar renewables in non-interconnected areas, in *Solar World Congress 2023* (ISES, New Delhi, India, 2023). <https://doi.org/10.18086/swc.2023.05.02>
11. Twinsolar, <https://twinsolar.eu/>
12. D.L. Guittet, J.M. Freeman, Tech. Rep. NREL/TP-6A20-7215 5, National Renewable Energy Laboratory (2018). <https://www.nrel.gov/docs/fy19osti/72155.pdf>
13. C. Long, E. Dutton, BSRN global network recommended QC tests, v2.0, (2002). [https://bsrn.awi.de/fileadmin/user\\_upload/bsrn.awi.de/Publications/BSRN\\_recommended\\_QC\\_tests\\_V2.pdf](https://bsrn.awi.de/fileadmin/user_upload/bsrn.awi.de/Publications/BSRN_recommended_QC_tests_V2.pdf)
14. A. Forstinger, S. Wilbert, A. Jensen, B. Kraas, C. Fernández Peruchena, C. Gueymard, D. Ronzio, D. Yang, E. Collino, J. Polo Martinez et al., Expert quality control of solar radiation ground data sets, in *ISES Solar World Congress* (online, France, 2021). <https://doi.org/10.18086/swc.2021.38.02>
15. A.R. Jensen, Y.M. Saint-Drenan, Quality assessment of solar irradiance data (2022). [https://assessingsolar.org/notebooks/quality\\_assessment.html](https://assessingsolar.org/notebooks/quality_assessment.html) [Accessed 13-09-2024]
16. A. Lenoir, F. Garde, Tropical NZEB, High Perform. Build. J. 43–55 (2012)
17. System Advisor Model Update Includes New Data, Improved Model Integration — nrel.gov. <https://www.nrel.gov/news/program/2020/system-advisor-model-update-includes-new-data-improved-model-integration.html> [Accessed 05-06-2024]
18. J.S. Stein, W.F. Holmgren, J. Forbess, C.W. Hansen, PVLIB: Open source photovoltaic performance modeling functions for Matlab and Python, in *2016 IEEE 43rd Photovoltaic Specialists Conference (PVSC)* (IEEE, 2016). <http://dx.doi.org/10.1109/PVSC.2016.7750303>
19. N. Blair, N. DiOrio, J. Freeman, P. Gilman, S. Janzou, T. Neises, M. Wagner, System advisor model (SAM) general description, technical report (version 2017. 9.5). <https://www.osti.gov/servlets/purl/1440404/>
20. K.S. Anderson, C.W. Hansen, W.F. Holmgren, A.R. Jensen, M.A. Mikofski, A. Driesse, pvlib python: 2023 project update, J. Open Source Softw. **8**, 5994 (2023). <http://dx.doi.org/10.21105/joss.05994>
21. A.P. Dobos, Pvwatts version 1 technical reference (2013). <https://www.nrel.gov/docs/fy14osti/60272.pdf>
22. A.P. Dobos, Pvwatts version 5 manual (2014). <https://www.osti.gov/biblio/1158421>
23. S. Pelland, J. Remund, J. Kliessl, O. Takashi, K. De Brandere, IEA PVPS T14-01, International Energy Agency (2013)
24. J.A. Kratochvil, W.E. Boyson, D.L. King, Photovoltaic array performance model, technical report (2004). <https://www.osti.gov/biblio/919131>
25. W. Short, D.J. Packey, T. Holt, *A manual for the economic evaluation of energy efficiency and renewable energy technologies*, repr. from the 1995 edn. (University Press of the Pacific, Honolulu, Hawaii, 2005). <https://www.nrel.gov/docs/legosti/old/5173.pdf>
26. J. Le Gal La Salle, M. David, P. Lauret, Finding the optimal size and design of microgrid energy system using genetic algorithm, in *41st European Photovoltaic Solar Energy Conference and Exhibition* (EU PVSEC, Vienna, Austria, 2024)

**Cite this article as:** Tina Arizo Randrianantenaina, Josselin Le Gal La Salle, Sergiu Viorel Spataru, Mathieu David, Increasing the self-sufficiency of a university campus by expanding the PV capacity while minimizing the energy cost, EPJ Photovoltaics **16**, 7 (2025)